DALTON
FULL PAPER

Syntheses, crystal structures and magnetic properties of polynuclear 1,4,5,8,9,12-hexaazatriphenylene (hat)-bridged copper(II) complexes

Hilde Grove,[a] Jorunn Sletten,*[a] Miguel Julve[b] and Francesc Lloret[b]

[a] *Department of Chemistry, University of Bergen, Allégaten 41, N-5007 Bergen, Norway*
[b] *Department of Inorganic Chemistry, Faculty of Chemistry, University of Valencia, Dr. Moliner 50, 46100 Burjassot (Valencia), Spain*

Received 1st December 2000, Accepted 9th February 2001
First published as an Advance Article on the web 8th March 2001

Three polynuclear compounds containing copper(II) and 1,4,5,8,9,12-hexaazatriphenylene (hat) as the basic building blocks have been prepared, $[Cu_4(hat)_2Cl_8]_n \cdot 6nH_2O$ **1**, $[Cu(hat)(H_2O)_2]_n[NO_3]_{2n}$ **2**, and $[Cu_2(hat)(H_2O)_6]_n[SO_4]_{2n} \cdot 2nH_2O$ **3**, their crystal structures determined and variable-temperature magnetic susceptibility data measured. The basic building block in **1** is the dinuclear $[Cu_2(hat)Cl_4]$ entity, two such units being connected to tetranuclear units through relatively strong axial Cu–Cl bonds (out-of-plane di-μ-chloro bridges). Weaker axial Cu · · · Cl interactions link the units into a sheet structure. In **2** and **3** hat-bridged copper(II) chains extending along glide planes are present. hat serves as a bis-bidentate ligand in **2** and as a ter-bidentate ligand in **3**; in the latter compound one of the copper atoms coordinated to hat does not participate in chain formation. The copper coordination geometries observed in these compounds are square pyramidal and elongated octahedral. hat coordinates either in only equatorial positions to copper (**1**), or alternates with one chelate in two equatorial positions and another in one equatorial and one axial position (**2** and **3**). The copper · · · copper distance across the hat bridge in **1** is 6.857(1) Å and 3.517(1), 3.600(1) and 3.651(1) Å across the three different di-μ-chloro bridges. In **2** the intrachain Cu · · · Cu distance is 6.797(1) Å. Three different Cu · · · Cu distances across the hat bridge are found in **3**, one of 6.789(1) Å involving two equatorial Cu–N bonds across a pyrazine ring, and two of 7.117(1) and 7.186(1) Å involving one equatorial and one axial Cu–N bond to a pyrazine. Variable-temperature susceptibility measurements on **1**–**3** reveal the occurrence of weak intramolecular antiferromagnetic interactions between copper(II) ions through bridging hat, the J values being −2.5 (**1**), −2.1 (**2**) and −2.4 cm^{-1} (**3**). In **1** the interaction across the di-μ-chloro bridge within the tetranuclear entity (J') is found to be weak and ferromagnetic in character (*ca.* +0.7 cm^{-1}).

Introduction

A ten-step synthetic procedure for preparing 1,4,5,8,9,12-hexaazatriphenylene (hat) was first published in 1981.[1a] A new, more simple procedure appeared in 1986,[1b] however, due to problems of low yield and expensive solvents and as the starting material was the explosive 1,3,5-triamino-2,4,6-trinitrobenzene, the production of this compound was rather limited. Publication of a straightforward synthesis of hat hexacarboxylic acid,[1c] which on decarboxylation yields the parent hat,[1d] has made this heterocycle more easily available in multigram quantities. hat dihydrate as well as some hexasubstituted derivatives of hat have been structurally characterized by X-ray crystallography.[2]

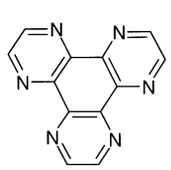

hat

hat is a potentially interesting ligand system; with its three sites for bidentate bonding to metal centres it can serve as a bidentate ligand in mononuclear complexes and as a bridging bis-bidentate and ter-bidentate ligand in di-, tri- and polynuclear compounds. The main body of studies on hat–metal compounds up to now has been concerned with electronic and photophysical properties of certain 4d and 5d complexes,[3] and of their interaction with polynucleotides.[4] Various substituted hat derivatives have been complexed with transition metal ions, and mononuclear,[5a] trinuclear,[5b] as well as polynuclear single cage and multicompartmental cage-type architectures[5c–e] have been structurally characterized. The latter type of compound exhibits anion inclusion in the cavities and anion exchange properties.[5e] Only one metal complex of hat itself, $[Ag(hat)]ClO_4 \cdot 2CH_3NO_2$, has been fully structurally characterized by X-ray crystallographic methods; the investigation revealed an interesting three-dimensional coordination polymer with ter-bidentate hat and chiral micropores, with the ability to exchange solvent without affecting the Ag–hat framework.[6]

In the present work we report the first syntheses, structure determinations and magnetic susceptibility studies of hat-bridged copper(II) complexes, the polynuclear $[Cu_4(hat)_2Cl_8]_n \cdot 6nH_2O$ **1**, $[Cu(hat)(H_2O)_2]_n[NO_3]_{2n}$ **2**, and $[Cu_2(hat)(H_2O)_6]_n[SO_4]_{2n} \cdot 2nH_2O$ **3**. We have previously reported on di-[7a] and poly-nuclear[7b] complexes of the related bridging ligand pyrazino[2,3-*f*][4,7]phenanthroline.

Experimental

Materials

1,4,5,8,9,12-Hexaazatriphenylene was prepared from 1,2,3,4,5,6-hexaoxocyclohexane by the method of Czarnik and co-workers.[1c,d] All other chemicals were purchased from commercial sources and used as received.

Preparations

$[Cu_4(hat)_2Cl_8]_n \cdot 6nH_2O$ 1. A mixture of 0.662 mmol (112.8 mg) of $CuCl_2 \cdot 2H_2O$ and 0.220 mmol (51.6 mg) of hat in 25 cm^3 of water was stirred for one hour at 80 °C. After slow cooling to room temperature the brown solution was filtered. Light green, irregularly shaped crystals of complex **1** appeared after slow

evaporation at room temperature. In order to ensure purity of the product the evaporation was stopped before precipitation was complete, at approximately 50% yield with respect to the hat present. The crystals are stable in air for several weeks (Found: C, 25.8; H, 2.3; N, 15.1. Calc. for $C_{12}H_{12}Cl_4Cu_2N_6O_3$: C, 25.9; H, 2.2; N, 15.1%).

$[Cu(hat)(H_2O)_2]_n[NO_3]_{2n}$ 2. 25 cm^3 of water were added to a mixture of 0.427 mmol (103.2 mg) of $Cu(NO_3)_2{\cdot}3H_2O$ and 0.213 mmol (50.0 mg) of hat. The solution was heated to 80 °C and stirred for two hours. The resulting brown solution was cooled to room temperature and filtered. Evaporation at room temperature afforded brown plate-formed crystals of complex **2**. The yield was 75% based on hat present. The crystals are stable in air for several months (Found: C, 31.5; H, 2.3; N, 24.4; O, 27.9. Calc. for $C_{12}H_{10}CuN_8O_8$: C, 31.5; H, 2.3; N, 24.5; O, 28.0%).

$[Cu_2(hat)(H_2O)_6]_n[SO_4]_{2n}{\cdot}2nH_2O$ 3. 0.640 mmol (159.9 mg) of $CuSO_4{\cdot}5H_2O$ and 0.213 mmol (50.0 mg) of hat were dissolved in 25 cm^3 of water under continuous stirring at 80 °C. After cooling to room temperature the brown solution was filtered. Brown needle-shaped crystals of complex **3** precipitated after slow evaporation at room temperature. The crystals are stable in air for several months. The yield was 85% based on hat present (Found: C, 20.7; H, 3.3; N, 12.0; O, 36.7; S, 9.2. Calc. for $C_6H_{11}CuN_3O_8S$: C, 20.7; H, 3.2; N, 12.1; O, 36.7; S, 9.2%).

Physical techniques

Infrared spectra were recorded with a Nicolet 800 FTIR spectrophotometer as KBr pellets in the 4000–400 cm^{-1} region. The magnetic susceptibilities of polycrystalline samples were measured over the temperature range 1.8–290 K with a Quantum Design SQUID susceptometer and using an applied magnetic field of 0.1 T. The complex $(NH_4)_2Mn(SO_4)_2{\cdot}6H_2O$ was used as a susceptibility standard. Diamagnetic corrections of the constituent atoms were estimated from Pascal's constants and found to be -586×10^{-6} (**1**), -213×10^{-6} (**2**), and -345×10^{-6} cm^3 mol^{-1} (**3**) per four (**1**), one (**2**) and two (**3**) copper(II) ions.[8] A value of 60×10^{-6} cm^3 mol^{-1} was used for the temperature-independent paramagnetism of the copper(II) ion.

Crystallography

Crystal parameters and refinement results are summarized in Table 1. Diffraction data were collected at 173 K using a SMART 2K CCD area detector diffractometer, equipped with an Oxford Cryostream N_2 cooling device.[9] The data collection covered a full sphere of reciprocal space for **1** and **3** and a hemisphere for **2**. Empirical absorption corrections were carried out (SADABS).[10] The structures were solved by direct methods (**1**) and the Patterson method (**2** and **3**), and were all refined by full-matrix least squares based on F^2 and including all reflections. All non-hydrogen atoms were refined anisotropically. Hydrogen atoms bound to carbon were included at idealized, calculated positions while water hydrogen atoms were located in Fourier difference maps. All hydrogen atoms were refined according to the riding model. For compound **1** the near identical lengths of the *b* and *c* axes indicates that a higher symmetry may be present. Metrically a monoclinic A-centred cell is possible. The internal agreement between symmetry equivalent reflections for such a cell is, however, very poor ($R_{int} = 0.64$), and the structure could not be solved with this choice of symmetry. The successful solution and refinement in space group $P\bar{1}$ shows conclusively that a higher symmetry is not present. For **3** the space group is not uniquely determined by the systematic extinctions. The non-centrosymmetric cell was chosen based on intensity statistics, and the solution and refinement revealed significant deviations from centrosymmetry in the structure.

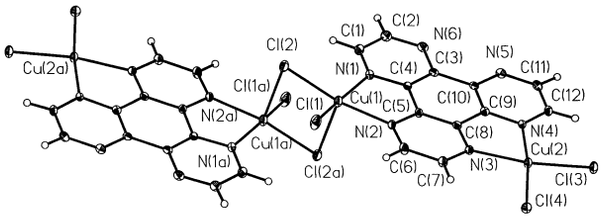

Fig. 1 The tetranuclear entity $[Cu_4(hat)_2Cl_8]$ in complex **1**. Thermal ellipsoids are plotted at the 30% probability level in all cases. Symmetry operation: (a) $-x + 2, -y + 1, -z$.

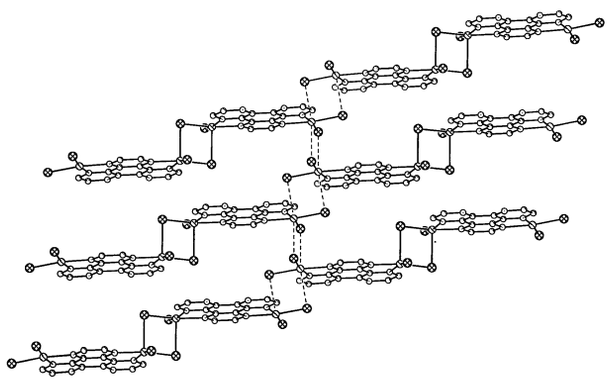

Fig. 2 Section of the sheet structure in complex **1** showing the hat- and chloro-bridged units.

The SMART and SAINT programs[11] were used for data collections and data integration. Structure solutions, refinements and graphics were performed with SHELXS 86, SHELXL-93 and XP.[12] Selected bond distances and angles are listed in Tables 2–4.

CCDC reference numbers 154056–154058.

See http://www.rsc.org/suppdata/dt/b0/b009647o/ for crystallographic data in CIF or other electronic format.

Results and discussion

Structures

$[Cu_4(hat)_2Cl_8]_n{\cdot}6nH_2O$ 1. The basic building block of this structure is the dinuclear $[Cu_2(hat)Cl_4]$ entity, where hat serves as a bis-bidentate ligand. A tetranuclear unit is defined through the out-of-plane di-μ-chloro bridge provided by Cl(2) (Fig. 1). These axial Cu–Cl bonds (Cu(1)–Cl(2a) = Cu(1a)–Cl(2) 2.664(1) Å) are among the shorter observed in di-μ-chloro-bridged copper(II) complexes.[13] Each such unit is further connected to two symmetry related neighbour units through somewhat weaker axial interactions (Cu(2)···Cl(4b) = Cu(2b)···Cl(4) = 2.810(1), Cu(2)···Cl(3c) = Cu(2c)···Cl(2) 2.860(1) Å; b $1 - x$, $2 - y$, $1 - z$; c $-x$, $2 - y$, $1 - z$) creating sheets with a staircase like appearance (Fig. 2). One of the crystal water molecules provides O–H···N and O–H···Cl hydrogen bonds between neighbour layers (O···N 3.007(4) Å, O–H···N 162°, O···Cl 3.283(3) Å, O–H···Cl 176°) while the two remaining water molecules form O–H···O and O–H···Cl hydrogen bonds within a layer (O···O 2.811(6) Å, O–H···O 165°, O···Cl 3.205(4)–3.431(5) Å, O–H···Cl 154–168°).

Taking into account all the axial Cu–Cl interactions, the coordination geometry of Cu(1) may be described as square pyramidal, and that of Cu(2) as elongated octahedral. The equatorial Cu–Cl bonds fall within the range 2.217(1) to 2.285(1) Å, the shortest bond being associated with the chlorine which is not bridging, and the longer one with the chlorine which forms the shortest axial interaction to a neighbour unit. All four Cu–N bonds are of similar lengths (2.051(3)–2.061(3)

Table 1 Summary of crystallographic data and structure refinement for $[Cu_4(hat)_2Cl_8]_n \cdot 6nH_2O$ **1**, $[Cu(hat)(H_2O)_2]_n[NO_3]_{2n}$ **2**, and $[Cu_2(hat)(H_2O)_6]_n[SO_4]_{2n} \cdot 2nH_2O$ **3**

	1	**2**	**3**
Formula	$C_{12}H_{12}Cl_4Cu_2N_6O_3$	$C_{12}H_{10}CuN_8O_8$	$C_{12}H_{22}Cu_2N_6O_{16}S_2$
M	557.16	457.82	697.56
Crystal system	Triclinic	Monoclinic	Orthorhombic
Space group	$P\bar{1}$	$P2_1/n$	$Pca2_1$
a/Å	6.7729(3)	9.3161(3)	13.5778(4)
b/Å	11.7016(5)	15.9239(4)	9.41490(10)
c/Å	11.7080(5)	10.1922(3)	17.8842(4)
α/°	85.725(2)		
β/°	78.736(2)	91.8540(10)	
γ/°	78.559(1)		
U/Å^3	891.33(7)	1511.21(8)	2286.20(9)
Z	2	4	4
μ/mm^{-1}	3.014	1.520	2.137
Reflections collected	12268	11379	31469
Unique reflections	3893 (R_{int} = 0.049)	3648 (R_{int} − 0.045)	5515 (R_{int} = 0.106)
R [$I > 2\sigma(I)$]	0.0398	0.0427	0.0427
R_w [$I > 2\sigma(I)$]	0.0761	0.0833	0.0698
R [all refl.]	0.0738	0.0726	0.0685
R_w [all refl.]	0.0877	0.0945	0.0772

Table 2 Selected bond lengths (Å) and angles (°) for $[Cu_4(hat)_2Cl_8]_n \cdot 6nH_2O$ **1**, with e.s.d.s in parentheses

Cu(1)–N(2)	2.051(3)	Cu(2)–N(4)	2.056(3)
Cu(1)–N(1)	2.059(3)	Cu(2)–N(3)	2.061(3)
Cu(1)–Cl(1)	2.2174(12)	Cu(2)–Cl(4)	2.2511(10)
Cu(1)–Cl(2)	2.2850(11)	Cu(2)–Cl(3)	2.2621(11)
Cu(1)–Cl(2a)	2.6636(12)	Cu(2) · · · Cl(4b)	2.8101(12)
		Cu(2) · · · Cl(3c)	2.8602(12)
N(2)–Cu(1)–N(1)	81.05(12)	N(3)–Cu(2)–Cl(3)	171.45(9)
N(2)–Cu(1)–Cl(1)	90.77(9)	Cl(4)–Cu(2)–Cl(3)	94.47(4)
N(1)–Cu(1)–Cl(1)	164.54(10)	N(4)–Cu(2)–Cl(4b)	87.33(9)
N(2)–Cu(1)–Cl(2)	170.95(9)	N(3)–Cu(2)–Cl(4b)	87.44(9)
N(1)–Cu(1)–Cl(2)	92.48(9)	Cl(4)–Cu(2)–Cl(4b)	88.33(4)
Cl(1)–Cu(1)–Cl(2)	94.03(4)	Cl(3)–Cu(2)–Cl(4b)	97.14(4)
N(2)–Cu(1)–Cl(2a)	96.42(9)	N(4)–Cu(2)–Cl(3c)	87.23(9)
N(1)–Cu(1)–Cl(2a)	89.01(9)	N(3)–Cu(2)–Cl(3c)	83.35(9)
Cl(1)–Cu(1)–Cl(2a)	105.01(4)	Cl(4)–Cu(2)–Cl(3c)	96.15(4)
Cl(2)–Cu(1)–Cl(2a)	89.75(4)	Cl(3)–Cu(2)–Cl(3c)	91.50(4)
N(4)–Cu(2)–N(3)	81.01(12)	Cl(4b)–Cu(2)–Cl(3c)	169.94(3)
N(4)–Cu(2)–Cl(4)	172.65(9)	Cu(1)–Cl(2)–Cu(1a)	90.25(4)
N(3)–Cu(2)–Cl(4)	92.87(9)	Cu(2)–Cl(4)–Cu(2b)	91.67(4)
N(4)–Cu(2)–Cl(3)	91.97(9)	Cu(2)–Cl(3)–Cu(2c)	88.50(4)

Symmetry transformations used to generate equivalent atoms: (a) $-x + 2, -y + 1, -z$; (b) $-x + 1, -y + 2, -z + 1$; (c) $-x, -y + 2, -z + 1$.

Å). The equatorial planes of both copper atoms have a small tetrahedral distortion (maximum atomic deviations 0.064 and 0.087 Å for Cu(1) and Cu(2), respectively). Cu(1) is displaced by 0.193 Å from the equatorial plane in the direction of the axial chlorine, while Cu(2) is situated approximately in the plane (Δ = 0.008 Å). The equatorial planes of the two copper atoms are oriented at 9.9° to each other and at 5.8 (Cu(1)) and 4.2° (Cu(2)) to the mean plane of the bridging hat ligand.

The copper–copper distance across the hat bridge is 6.857(1) Å, while across the chloro bridges the distances are 3.517(1) (across Cu(1)–Cl(2) · · · Cu(1a), the bond angle at Cl(2) being 90.25(4)°), 3.600(1) (across Cu(2)–Cl(3) · · · Cu(2c), the bond angle at Cl(3) being 88.50(4)°) and 3.651(1) Å (across Cu(2)–Cl(4) · · · Cu(2b), the bond angle at Cl(4) being 91.67(4)°.

$[Cu(hat)(H_2O)_2]_n[NO_3]_{2n}$ 2. In this compound $[Cu(hat)(H_2O)_2]^{2+}$ units are linked into chains through the *n*-glide operation, hat serving as a bridging, bis(bidentate) ligand, and the Cu · · · Cu · · · Cu sequence being almost linear (175.7°) (Fig. 3). The copper atom has elongated, octahedral geometry with two nitrogen atoms from one hat, one nitrogen atom from another and a water molecule in axial positions (N(1), N(2), N(3a), O(1)), and a hat nitrogen atom and a water molecule in axial positions. The equatorial plane of copper has a small tetrahedral distortion (maximum atomic deviation 0.108 Å) with copper situated approximately in the plane (Δ = 0.006 Å). The equatorial planes of two neighbour copper atoms along the chain are oriented at 89.7° to each other, and the copper equatorial plane makes angles of 8.2° to the hat plane on one side and of 83.7° on the other. The planes of two neighbour hat units are oriented at 76.7° to each other.

The intra-chain copper–copper distance across the hat bridge is 6.797(1) Å, while the shortest inter-chain metal–metal distance is 7.019(1) Å. Neighbour chains are connected to double layer sheets through weak hydrogen bonds between the axial water and one of the uncoordinated hat nitrogen atoms (O · · · N 3.097(3) Å, O–H · · · N 173°). The nitrate counter ions are involved in hydrogen bonds to the coordinated water molecules and thus provide links both within and between the double layers (O · · · O 2.704(3)–2.925(3) Å, O–H · · · O 175–177°).

$[Cu_2(hat)(H_2O)_6]_n[SO_4]_{2n} \cdot 2nH_2O$ 3. $[Cu_2(hat)(H_2O)_6]^{4+}$ units are linked into chains through the *a*-glide operation (Fig. 4). hat is in this case serving as a ter-bidentate ligand, but one of the copper atoms, Cu(2), does not participate in chain formation. Also in this case the Cu · · · Cu · · · Cu sequence is close to linear (178.8°), and the general features of the chain are similar to those found in compound **2**. Cu(1) has elongated, octahedral

Table 3 Selected bond lengths (Å) and angles (°) for $[Cu(hat)(H_2O)_2]_n[NO_3]_{2n}$ **2** with e.s.d.s

Cu(1)–O(1)	1.997(2)	Cu(1)–N(1)	2.069(2)
Cu(1)–N(2)	2.037(2)	Cu(1)–N(4a)	2.277(3)
Cu(1)–N(3a)	2.044(2)	Cu(1)–O(2)	2.302(2)
O(1)–Cu(1)–N(2)	90.73(9)	N(3a)–Cu(1)–N(4a)	78.15(9)
O(1)–Cu(1)–N(3a)	89.21(9)	N(1)–Cu(1)–N(4a)	93.96(9)
N(2)–Cu(1)–N(3a)	174.64(10)	O(1)–Cu(1)–O(2)	87.90(8)
O(1)–Cu(1)–N(1)	170.05(9)	N(2)–Cu(1)–O(2)	92.50(9)
N(2)–Cu(1)–N(1)	81.66(10)	N(3a)–Cu(1)–O(2)	92.86(9)
N(3a)–Cu(1)–N(1)	98.96(9)	N(1)–Cu(1)–O(2)	86.04(9)
O(1)–Cu(1)–N(4a)	93.27(9)	N(4a)–Cu(1)–O(2)	170.91(8)
N(2)–Cu(1)–N(4a)	96.50(9)		

Symmetry transformations used to generate equivalent atoms: (a) $x - \frac{1}{2}$, $-y + \frac{1}{2}$, $z - \frac{1}{2}$.

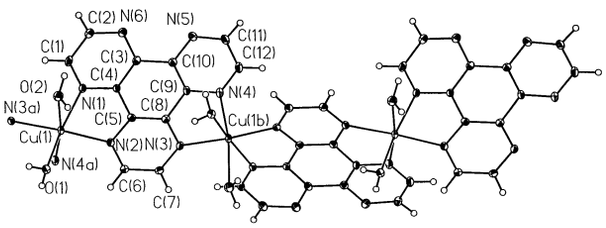

Fig. 3 Section of the $[Cu(hat)(H_2O)_2]_n^{2n+}$ chain in complex **2**. Symmetry operations: (a) $x - \frac{1}{2}$, $-y + \frac{1}{2}$, $z - \frac{1}{2}$; (b) $x + \frac{1}{2}$, $-y + \frac{1}{2}$, $z + \frac{1}{2}$.

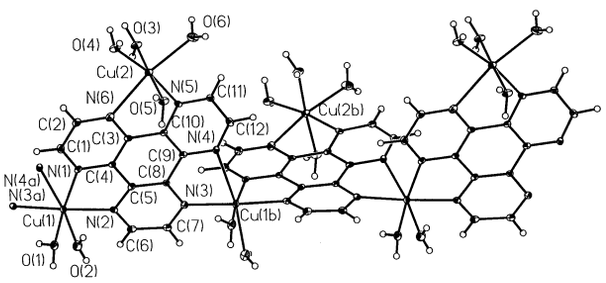

Fig. 4 Section of the $[Cu_2(hat)(H_2O)_6]_n^{4n+}$ chain in complex **3**. Symmetry operations: (a) $x - \frac{1}{2}$, $-y + 1$, z; (b) $x + \frac{1}{2}$, $-y + 1$, z.

geometry with two nitrogen atoms from one hat, one nitrogen atom from another and a water molecule in axial positions (N(1), N(2), N(3a), O(1)), and a hat nitrogen atom and a water molecule in axial positions. The equatorial plane of copper has no significant distortion (maximum atomic deviation 0.013 Å) with copper displaced slightly from the plane ($\Delta = 0.050$ Å) in the direction towards the axial water molecule. The equatorial planes of two neighbour copper atoms along the chain are oriented at 73.1° to each other, and the copper equatorial plane makes angles of 4.8° to the hat plane on one side and of 77.3° on the other. The planes of two neighbour hat units are oriented at 81.5° to each other. The Cu(2) atom also has an elongated octahedral coordination geometry. In this case one hat nitrogen and three water molecules define the equatorial plane (N(5), O(3), O(4), O(5)), and another hat nitrogen atom and a water molecule are situated in axial positions.

The intra-chain Cu(1)···Cu(1b) distance across the hat bridge is 6.789(1) Å, while the distances involving Cu(2) are somewhat longer, Cu(1)···Cu(2) 7.117(1), Cu(1b)···Cu(2) 7.186(1) Å. The shortest inter-chain metal–metal distances are 6.804(1) and 6.908(1) Å. The chains are connected through an extensive hydrogen bond network involving coordinated and uncoordinated water and sulfate counter ions (O···O 2.600(5)–2.994(5) Å, O–H···O 157–174°). The counter ions reside in channels running through the crystal lattice parallel to the chain axes.

Table 4 Selected bond lengths (Å) and bond angles (°) for $[Cu_2(hat)(H_2O)_6]_n[SO_4]_{2n}\cdot 2nH_2O$ **3** with e.s.d.s in parentheses

Cu(1)–O(1)	1.946(3)	Cu(2)–O(4)	1.948(3)
Cu(1)–N(3a)	2.033(3)	Cu(2)–O(3)	1.998(3)
Cu(1)–N(1)	2.035(4)	Cu(2)–O(5)	2.000(3)
Cu(1)–N(2)	2.039(3)	Cu(2)–N(5)	2.055(4)
Cu(1)–O(2)	2.319(3)	Cu(2)–O(6)	2.253(3)
Cu(1)–N(4a)	2.445(4)	Cu(2)–N(6)	2.404(4)
O(1)–Cu(1)–N(3a)	91.18(13)	O(4)–Cu(2)–O(3)	93.45(13)
O(1)–Cu(1)–N(1)	172.41(15)	O(4)–Cu(2)–O(5)	90.56(13)
N(3a)–Cu(1)–N(1)	95.44(14)	O(3)–Cu(2)–O(5)	175.98(13)
O(1)–Cu(1)–N(2)	91.03(13)	O(4)–Cu(2)–N(5)	170.58(15)
N(3a)–Cu(1)–N(2)	176.9(2)	O(3)–Cu(2)–N(5)	87.57(14)
N(1)–Cu(1)–N(2)	82.22(14)	O(5)–Cu(2)–N(5)	88.51(14)
O(1)–Cu(1)–O(2)	95.58(14)	O(4)–Cu(2)–O(6)	98.49(13)
N(3a)–Cu(1)–O(2)	94.71(14)	O(3)–Cu(2)–O(6)	90.38(13)
N(1)–Cu(1)–O(2)	87.59(13)	O(5)–Cu(2)–O(6)	88.76(13)
N(2)–Cu(1)–O(2)	87.30(13)	N(5)–Cu(2)–O(6)	90.86(13)
O(1)–Cu(1)–N(4a)	88.37(13)	O(4)–Cu(2)–N(6)	94.04(13)
N(3a)–Cu(1)–N(4a)	75.63(13)	O(3)–Cu(2)–N(6)	88.58(13)
N(1)–Cu(1)–N(4a)	89.68(14)	O(5)–Cu(2)–N(6)	91.41(13)
N(2)–Cu(1)–N(4a)	102.20(13)	N(5)–Cu(2)–N(6)	76.62(14)
O(2)–Cu(1)–N(4a)	169.67(12)	O(6)–Cu(2)–N(6)	167.46(13)

Symmetry transformations used to generate equivalent atoms: (a) $x - \frac{1}{2}$, $-y + \frac{1}{2}$, z.

The bridging hat ligand. The bridging hat ligand in complexes **1** and **2** deviates only slightly from planarity, the maximum atomic deviations being 0.049 (**1**) and 0.060 Å (**2**), and the corresponding mean deviations being 0.020 and 0.026 Å, respectively. This is comparable to the situation observed in the crystal structure of uncomplexed hat (maximum atomic deviation 0.070 Å, mean deviation 0.035 Å).[2a] A slight decrease in the average of the N–C–C angles within the chelate rings in **1** and **2** as compared to that found in hat itself is compensated by an increase in the corresponding angles involving N(5) and N(6) where metal is not bonded. In complex **3**, however, the ter-bidentate coordination evidently causes more strain to the bridging hat molecule; here the maximum atomic deviation is 0.191 Å and the mean deviation 0.103 Å. The N–C bond lengths are only marginally affected by the metal coordination. The most consistent bond lengths changes upon complexation occur in the phenylene ring, where the average bond length has decreased by 0.013 (**1**), 0.010 (**2**) and 0.015 Å (**3**) as compared to that of free hat. These features are in agreement with those observed when comparing the related pyrazino[2,3-*f*][4,7]phenanthroline (pap) complexes to uncomplexed pap.[2a]

Infrared spectra

The free hat ligand shows a number of strong peaks in the 1500 to 1000 cm^{-1} region; 1468 (sharp, s), 1376 (with shoulder, s), 1327 (sharp, s), 1229 (sharp, s) and 1098 cm^{-1} (sharp, s). In the spectrum of complex **1** it is clearly seen that all these peaks are shifted to higher wavenumbers on complex formation (Δ ranging from 5 to 21 cm^{-1}). This is consistent with metal coordination of the nitrogen atoms of the aromatic rings.[14] The presence of nitrate and sulfate in the spectra of **2** and **3** is evidenced by broad, strong features centred around 1385 and 1121 cm^{-1}, respectively. In the portion of the spectra that is not obscured by the strong absorptions of the anions one can observe shifts in the aromatic ring vibrations in the same order of magnitude as those observed for complex **1**.

Magnetic properties

The magnetic properties of the complexes **1**–**3** in the form of both χ_m and $\chi_m T$ *versus* T plots are shown in Figs. 5–7, χ_m being the magnetic susceptibility per four (**1**), one (**2**) and two (**3**)

copper(II) ions. The values of $\chi_m T$ at room temperature are 1.60 (**1**), 0.42(**2**) and 0.82 cm^3 K mol^{-1} (**3**), and they are as expected for four (**1**), one (**2**) and two (**3**) magnetically non-interacting spin doublets. These values remain practically constant upon cooling until 30 K and then decrease sharply at lower temperatures, attaining values of 0.14 (**1**), 0.17 (**2**) and 0.55 cm^3 K mol^{-1} (**3**). These features are characteristic of the presence of weak antiferromagnetic interactions. An incipient maximum of the magnetic susceptibility is observed at 2.2 K for **1** and at 1.9 K for **2** whereas no maximum occurs in the susceptibility curve of **3**.

In the light of the previous structural discussion of this series of compounds, we interpreted the magnetic behaviour of **1** through a tetranuclear model (see Fig. 1) with the spin Hamiltonian (1)[15a] in which J and J' are the exchange coupling

$$\hat{H} = -J(\hat{S}_1\hat{S}_2 + \hat{S}_3\hat{S}_4) - J'\hat{S}_2\hat{S}_3 \quad (1)$$

constants across hat (between Cu(1) and Cu(2)) and across the double chloro bridge, Cl(2)/Cl(2a), (between Cu(1) and Cu(1a)), respectively. The resulting spin states and their corresponding energies are given in eqns. (2)–(6).

$$S_1 = 2 \quad E_1 = -(J/2) - (J'/4) \quad (2)$$

$$S_2 = 1 \quad E_2 = (J/2) - (J'/4) \quad (3)$$

$$S_3 = 1 \quad E_3 = (J'/4) + [(J^2 + J'^2)^{1/2}/2] \quad (4)$$

$$S_4 = 1 \quad E_4 = (J'/4) - [(J^2 + J'^2)^{1/2}/2] \quad (5)$$

$$S_5 = 0 \quad E_5 = (J/2) + (J'/4) + [(4J^2 - 2JJ' + J'^2)^{1/2}/2] \quad (6)$$

$$S_6 = 0 \quad E_6 = (J/2) + (J'/4) - [(4J^2 - 2JJ' + J'^2)^{1/2}/2] \quad (7)$$

The fit of the magnetic data by the appropriate susceptibility expression derived from the Van Vleck formula assuming that the g factors for both copper(II) ions are identical leads to $J = -2.5$ cm^{-1}, $J' = +0.7$ cm^{-1}, $g = 2.07$ and $R = 3.10 \times 10^{-5}$ (R is the agreement factor defined as $\Sigma_i[(\chi_m T)_{obs(i)} - (\chi_m T)_{calc(i)}]^2/\Sigma_i[(\chi_m T)_{obs(i)}]^2$). The calculated curve matches very well the magnetic data. The quality of the fit does not depend significantly on the value of J' and a quite good fit can be obtained through a simple Bleaney–Bowers expression for a copper(II) dimer,[15b] the value of the computed J being practically the same as for the previous model. The weak antiferromagnetic coupling through bridging hat is thus the dominant one, the magnetic interactions through the di-μ-chloro bridges within the tetranuclear unit and through the even longer out-of-plane Cu(2)···Cl(4b) and Cu(2)···Cl(3c) bonds being practically negligible.

Given that the structure of complex **2** consists of uniformly spaced chains of copper(II) ions bridged by bis-bidentate hat, its magnetic data have been analysed through the theoretical expression (the Hamiltonian being $\hat{H} = -J\Sigma\hat{S}_i\hat{S}_{i+1}$) proposed by Hall[15c] for a uniform chain of local spins $S = 1/2$, eqn. (8)

$$\chi_m = (N\beta^2 g^2/kT)[(0.25 + 0.14995x + 0.30094x^2)/(1 + 1.9862x + 0.68854x^2 + 6.0626x^3)] \quad (8)$$

where N, β and g have their usual meaning, $x = |J|/kT$ and J is the exchange coupling constant describing the magnetic interaction between two nearest-neighbour spin doublets. This expression, which derives from the numerical results of Bonner and Fisher,[15d] has been widely used for the analysis of magnetic data of uniform copper(II) chains. Least-squares fit of the magnetic data of **2** through eqn. (8) leads to $J = -2.1$ cm^{-1}, $g = 2.16$ and $R = 4.0 \times 10^{-5}$. The theoretical curve reproduces well the susceptibility data.

As far as the treatment of the magnetic data of complex **3** is concerned, one can see that the structure of this complex is made up of chains of hat-bridged triangles of copper(II) ions (denoted Cu(1), Cu(2) and Cu(1b)); neighbour triangles share the vertexes occupied by the symmetry-related copper atoms (see Fig. 5). No theoretical model for the spin topology that will result from a chain of triangles in which the magnetic interaction through all three edges is operative has been developed. However, a closer look at the structural features and

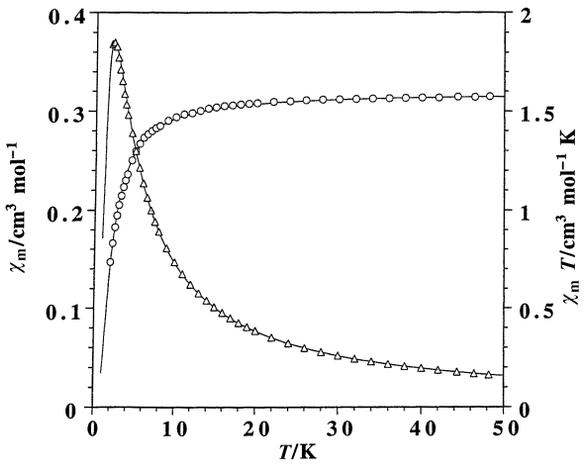

Fig. 5 Thermal dependence of χ_m (Δ) and $\chi_m T$ (○) for complex **1**: (Δ, ○) experimental data; (−) best fit through eqn. (1).

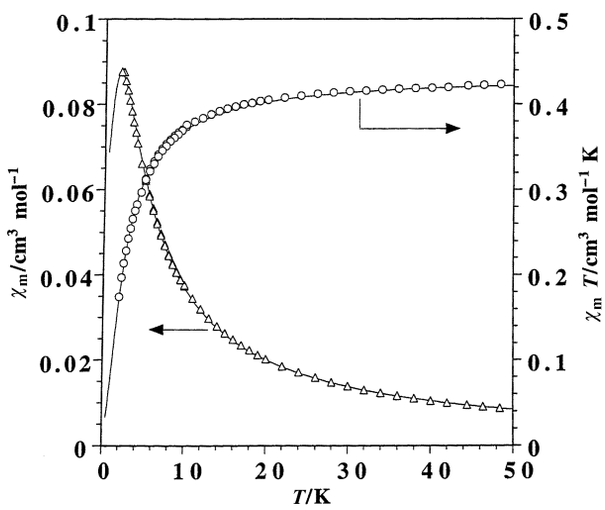

Fig. 6 Thermal dependence of χ_m (Δ) and $\chi_m T$ (○) for complex **2**: (Δ, ○) experimental data; (−) best fit through eqn. (8).

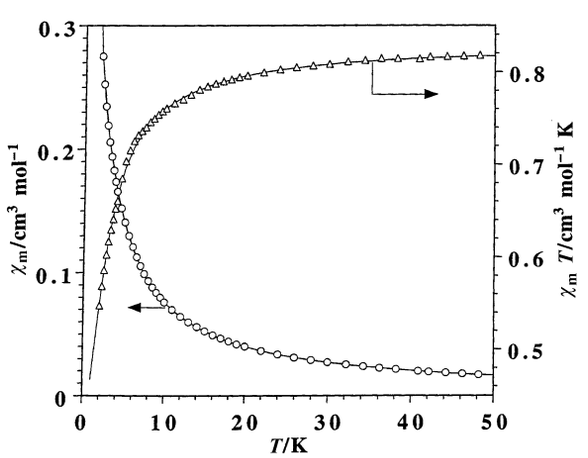

Fig. 7 Thermal dependence of χ_m (Δ) and $\chi_m T$ (○) for complex **3**: (Δ, ○) experimental data; (−) best fit through eqn. (9).

the orientations of the magnetic orbitals in **3** reveals that the situation in the present case is more simple. The copper(II) ions exhibit elongated octahedral surroundings, and the magnetic orbitals are roughly defined by the short equatorial bonds involving N(1), N(2), N(3a), O(1) at Cu(1) and N(5), O(3), O(4), O(5) at Cu(2) (Fig. 4). It is hence only the pathway through the pyrazine ring that bridges the two symmetry-related copper atoms (Cu(1) and Cu(1b)) which involves two short equatorial Cu–N bonds, and which is to be expected to sustain a significant magnetic interaction. Consequently, the magnetic behaviour of **3** was analysed through the expression for a uniformly spaced copper(II) chain [15c,d] plus an isolated spin doublet (Cu(2)) (eqn. (9)) where J is the intrachain exchange coupling constant, and g_1 and g_2 are the Lande factors for Cu(1) and Cu(2), respectively. Least-squares fit through this expression leads to $J = -2.4$ cm^{-1}, $g_1 = 2.17$, $g_2 = 2.07$ and $R = 8.7 \times 10^{-6}$.

$$\chi_m = (N\beta^2 g_1^2/kT)[(0.25 + 0.14995x + 0.30094x^2)/(1 + 1.9862x + 0.68854x^2 + 6.0626x^3)] + (N\beta^2 g_2^2/4kT) \quad (9)$$

Several points deserve to be pointed out in the light of the results reported in this work. The first concerns its novelty given that, as far as we are aware, this is the first magneto-structural study dealing with hat-bridged metal complexes. Secondly, our data reveal that the magnetic interaction between copper(II) ions separated by *ca*. 6.8 Å through bridging hat is very weak and antiferromagnetic in nature, the value of the coupling constant being −2.5 (**1**), −2.1 (**2**) and −2.4 cm^{-1} (**3**), respectively. The small overlap between the metal centred magnetic orbitals through the pyrazine fragment Cu(1)N(2)C(5)C(6)C(7)C(8)N(3)Cu(2)(**1**)/Cu(1b) (**2** and **3**) accounts for the weak magnetic coupling observed for each of the compounds. The fact that in **1** the magnetic orbitals on copper on both sides of the hat bridge are approximately coplanar with the hat plane, while in **2** and **3** the magnetic orbital on copper is coplanar with hat on one side of the bridge but close to normal to the hat plane on the other side, does not seem to have a significant effect on the size of the magnetic exchange parameter, confirming that it is the shortest pathway through a single pyrazine ring that is decisive in determining the interaction. The magnitude of the antiferromagnetic coupling in **1**–**3** compares well with values we have reported for related pap-bridged copper(II) complexes ($-J = 1.3$–2.5 cm^{-1}).[7] Thirdly, simple orbital symmetry considerations allowed us to model the magnetic behaviour of complex **3** through eqn. (9). The lack of a susceptibility maximum in the magnetic plot of **3** is due to the presence of a Curie tail for the magnetically non-interacting Cu(2). In addition, no plateau of $\chi_m T$ for the complexes could be observed in the low temperature region because of the weakness of the intrachain antiferromagnetic coupling. The last point concerns the very weak ferromagnetic interaction between copper(II) ions through the out-of-plane di-μ-chloro skeleton (Cu(1)Cl(2)Cl(2a)Cu(1a) fragment) in complex **1**. The magnetic orbital on Cu(1) is mainly located in the equatorial plane (N(1)N(2)Cl(1)Cl(2) set of atoms) and the spin density on its axial position (Cl(2a) atom with Cu(1)–Cl(2a) 2.664(1) Å) is expected to be very small. The poor overlap between the parallel magnetic orbitals centred on Cu(1) and Cu(1a) and the large metal–metal separation (Cu(1)···Cu(1a) 3.517 Å) suggest that only a weak magnetic coupling is to be expected, ferro- or antiferro-magnetic in character, due to the near orthogonality of the magnetic orbitals. A number of di-μ-chloro-bridged copper(II) dimeric and chain compounds have been structurally and magnetically characterized,[13] but no simple magneto-structural relationship relating the value of J to *e.g.* bonding angle at the chlorine, Cu–Cl or Cu···Cu distance has been established.

Acknowledgements

Thanks are due to Dr E. Bakstad and Mr K. F. Alnes for synthesizing 1,4,5,8,9,12-hexaazatriphenylene (the hat ligand). Grants from NFR (Research Council of Norway) and the University of Bergen allowing the purchase of X-ray equipment, a Ph.D.-student fellowship (H. G.) from the University of Bergen, as well as partial financial support (M. J. and F. L.) from the Spanish Dirección General de Investigación Científica y Técnica through project PB97-1397 is acknowledged.

References

1 (*a*) R. Nasielski-Hinkens, M. Benedek-Vamos, D. Maetens and J. Nasielski, *J. Organomet. Chem.*, 1981, **217**, 179; (*b*) D. Z. Rogers, *J. Org. Chem.*, 1986, **51**, 3904; (*c*) J. T. Rademacher, K. Kanakarajan and A. W. Czarnik, *Synthesis*, 1994, 378; (*d*) M. S. P. Sarma and A. W. Czarnik, *Synthesis*, 1988, 72.

2 (*a*) H. Grove and J. Sletten, *J. Chem. Crystallogr.*, 2000, **30**, 123; (*b*) J. C. Beeson, A. W. Czarnik, L. J. Fitzgerald and R. E. Gerkin, *Acta Crystallogr., Sect. C*, 1996, **52**, 724; (*c*) J. C. Beeson, L. J. Fitzgerald, J. C. Gallicci, R. E. Gerkin, J. T. Rademacher and A. W. Czarnik, *J. Am. Chem. Soc.*, 1994, **116**, 4621.

3 T. J. Rutherford and F. R. Keene, *J. Chem. Soc., Dalton Trans.*, 1998, 1155; T. J. Rutherford, O. Van Gitje, A. Kirsch-De Mesmaeker and F. R. Keene, *J. Chem. Soc., Dalton Trans.*, 1997, 4465; I. Ortmans, P. Didier and A. Kirsch-De Mesmaeker, *Inorg. Chem.*, 1995, **34**, 3695; P. Didier, I. Ortmans and A. Kirsch-De Mesmaeker, *Inorg. Chem.*, 1993, **32**, 5239; L. Jacquet and A. Kirsch-De Mesmaeker, *J. Chem. Soc., Faraday Trans.*, 1992, 2471; A. Kirsch-De Mesmaeker, L. Jacquet, A. Masschelein, F. Vanhecke and K. Heremans, *Inorg. Chem.*, 1989, **28**, 2465; R. Sahai, D. P. Rillema, R. Shaver, S. Van Wallendael, D. C. Jackman and M. Boldaji, *Inorg. Chem.*, 1989, **28**, 1022.

4 A. Kirsch-De Mesmaeker and S. Choua, *Inorg. Chem.*, 1997, **36**, 584; M. Casu, G. Saba, A. Lai, M. Luhmer, A. Kirsch-De Mesmaeker, C. Moucheron and J. Reisse, *Biophys. Chem.*, 1996, **59**, 133; J.-P. Lecomte, A. Kirsch-De Mesmaeker, M. M. Feeney and J. M. Kely, *Inorg. Chem.*, 1995, **34**, 6481; J.-P. Lecomte, A. Kirsch-De Mesmaeker and G. Orellana, *J. Phys. Chem.*, 1994, **98**, 5382; J.-P. Lecomte, A. Kirsch-De Mesmaeker, J. M. Kelly, A. Tossi and H. Gorner, *Photochem. Photobiol.*, 1992, **55**, 681.

5 (*a*) V. J. Catalano, W. E. Larson, M. M. Olmstead and H. B. Gray, *Inorg. Chem.*, 1994, **33**, 4502; (*b*) T. Okubo, S. Kitagawa, M. Kondo, H. Matsuzaka and T. Ishii, *Angew. Chem., Int. Ed.*, 1999, **38**, 931; (*c*) P. N. W. Baxter, J.-M. Lehn, G. Baum and D. Fenske, *Chem. Eur. J.*, 1999, **5**, 102; (*d*) P. Baxter, J.-M. Lehn, A. DeCian and J. Fischer, *Angew. Chem., Int. Ed. Engl.*, 1993, **32**, 69; (*e*) P. N. W. Baxter, J.-M. Lehn, B. O. Kneisel, G. Braum and D. Fenske, *Chem. Eur. J.*, 1999, **5**, 113.

6 B. F. Abrahams, P. A. Jackson and Richard Robson, *Angew. Chem., Int. Ed.*, 1998, **37**, 2656.

7 (*a*) H. Grove, J. Sletten, M. Julve and F. Lloret, *J. Chem. Soc., Dalton Trans.*, 2000, 515; (*b*) H. Grove, J. Sletten, M. Julve, F. Lloret and J. Cano, *J. Chem. Soc., Dalton Trans.*, 2001, 259.

8 A. Earnshaw, in *Introduction to Magnetochemistry*, Academic Press, London, 1968.

9 J. Cosier and F. H. Glazer, *J. Appl. Crystallogr.*, 1986, **19**, 105.

10 G. M. Sheldrick, SADABS, Empirical Absorption Correction Program, University of Göttingen, 1996, V 2.01.

11 SMART, Version 4.0, Data Collection Software; SAINT, Version 4.0, Data Integration Software; Bruker AXS, Inc., Madison, WI, 1997.

12 G. M. Sheldrick, *Acta Crystallogr., Sect. A*, 1990, **46**, 467; G. M. Sheldrick, SHELXL 93, University of Göttingen, 1993; XP, Version 4.3, Siemens Analytical X-ray Inst. Inc., Madison, WI, 1992.

13 M. Hernández-Molina, J. González-Platas, C. Ruiz-Pérez, F. Lloret and M. Julve, *Inorg. Chim. Acta*, 1999, **284**, 258, and references therein.

14 J. R. Allan, N. D. Baird and A. L. Kassyk, *J. Therm. Anal.*, 1979, **16**, 79.

15 (*a*) G. V. Rubenacker, J. E. Drumheller, K. Emerson and R. D. Willet, *J. Magn. Mater.*, 1986, **54**–**57**, 1483; (*b*) B. Bleaney and K. D. Bowers, *Proc. R. Soc. London, Ser. A*, 1952, **214**, 451; (*c*) J. W. Hall, Ph.D. Dissertation, University of North Carolina, Chapel Hill, NC, 1977; (*d*) J. C. Bonner and M. E. Fisher, *Phys. Rev. A*, 1964, **135**, 640.